Plant Molecular Biology (2018) 96:305–314
https://doi.org/10.1007/s11103-017-0696-3

Salt tolerance of two perennial grass *Brachypodium sylvaticum* accessions

Nir Sade[1] · Maria del Mar Rubio Wilhelmi[1] · Xiaojuan Ke[1] · Yariv Brotman[2] · Matthew Wright[1] · Imran Khan[1,5] · Wagner De Souza[1] · Elias Bassil[1] · Christian M. Tobias[3] · Roger Thilmony[3] · John P. Vogel[4] · Eduardo Blumwald[1]

Received: 19 October 2017 / Accepted: 27 December 2017 / Published online: 10 January 2018

Abstract

Key message **We studied the salt stress tolerance of two accessions isolated from different areas of the world (Norway and Tunisia) and characterized the mechanism(s) regulating salt stress in *Brachypodium sylvaticum* Osl1 and Ain1.**

Abstract Perennial grasses are widely grown in different parts of the world as an important feedstock for renewable energy. Their perennial nature that reduces management practices and use of energy and agrochemicals give these biomass crops advantages when dealing with modern agriculture challenges such as soil erosion, increase in salinized marginal lands and the runoff of nutrients. *Brachypodium sylvaticum* is a perennial grass that was recently suggested as a suitable model for the study of biomass plant production and renewable energy. However, its plasticity to abiotic stress is not yet clear. We studied the salt stress tolerance of two accessions isolated from different areas of the world and characterized the mechanism(s) regulating salt stress in *B. sylvaticum* Osl1, originated from Oslo, Norway and Ain1, originated from Ain-Durham, Tunisia. Osl1 limited sodium transport from root to shoot, maintaining a better K/Na homeostasis and preventing toxicity damage in the shoot. This was accompanied by higher expression of *HKT8* and *SOS1* transporters in Osl1 as compared to Ain1. In addition, Osl1 salt tolerance was accompanied by higher abundance of the vacuolar proton pump pyrophosphatase and Na^+/H^+ antiporters (NHXs) leading to a better vacuolar pH homeostasis, efficient compartmentation of Na^+ in the root vacuoles and salt tolerance. Although preliminary, our results further support previous results highlighting the role of Na^+ transport systems in plant salt tolerance. The identification of salt tolerant and sensitive *B. sylvaticum* accessions can provide an experimental system for the study of the mechanisms and regulatory networks associated with stress tolerance in perennials grass.

Keywords *Brachypodium* · Salt tolerance · Ion homeostasis · Perennial grass · Biomass crops

Introduction

Perennial grasses had been used traditionally as forage, turf and feedstock crops and during the last 20 years, they became a valuable source of renewable energy (McLaughlin and Kszos 2005). Perennial grasses hold great potential and some advantages over annual crops (Glover et al. 2010). Perennials can accumulate more biomass than annuals because of their longer growing seasons and their deeper rooting depths that allow them to retain and use more precipitation (Glover and Reganold 2010). In addition, due to their longer photosynthetic seasons, perennials have higher light interception efficiency that results in higher plant productivity. Because of their deep and extended root system, perennials maintain an efficient root water homeostasis and accumulate higher nutrients in their roots, thus reducing the need of frequent fertilization (Glover and Reganold 2010). Finally,

Electronic supplementary material The online version of this article (https://doi.org/10.1007/s11103-017-0696-3) contains supplementary material, which is available to authorized users.

✉ Eduardo Blumwald
eblumwald@ucdavis.edu

[1] Department of Plant Sciences, University of California, 1 Shields Ave, Mail Stop 5, Davis, CA 95616, USA

[2] Department of Life Sciences, Ben Gurion University of the Negev, Beersheva, Israel

[3] Western Regional Research Center, United States Department of Agriculture, Agricultural Research Service, Albany, CA, USA

[4] DOE Joint Genome Institute, 2800 Mitchell Dr., Walnut Creek, CA 94598, USA

[5] Department of Agronomy, University of Agriculture, Faisalabad, Pakistan

perennials contribute to a decreased soil erosion and an increased soil organic matter content. All these advantages have made perennial grasses as switchgrass and *Miscanthus* leading candidates for biomass and biofuel production and they are predicted to account for approximately 16 billion gallons of renewable fuels by the year 2022 (Carroll and Somerville 2009; Dohleman and Long 2009).

In general, the perennial grasses species targeted for biomass production are difficult experimentally because of their large size, slow generation time, complex genetics and difficulties in their genetic transformation (Lu et al. 2013; Yan et al. 2012). Thus, the development of a model perennial grass that could be easily grown and is amenable to genetic transformation would be most useful for the development of transgenic methodologies for crop biomass improvement. *Brachypodium sylvaticum*, a perennial grass from the *Poaceae* family, has been recently proposed as a suitable model for perennial grasses (Steinwand et al. 2013; Gordon et al. 2016). *B. sylvaticum* possesses all the traits necessary in a model system; it is mostly self-fertile and relatively small, with mature plants ranging from 35 to 70 cm. Despite its perennial nature; some accessions can go from seed to seed in approximately 3–4 months with no need of vernalization. It is a diploid with a relatively small genome with simple growth requirements. A transformation protocol for *B. sylvaticum* accession Ain1 has been established (Steinwand et al. 2013) and the full genome and transcriptome gene atlas is being developed (John Vogel, personal communication). Moreover, the close relationship between *B. sylvaticum* and the annual grass *Brachypodium distachyon* (used as a model plant for annual grasses) will facilitate to leverage the resources developed for the annual *B. distachyon* (Brkljacic et al. 2011).

The increasing production of second generation non-food bioenergy crops has raised concerns about the competition for cropland use between bioenergy production and food crops production. A viable solution to this problem is the development of stress-tolerant bioenergy crops, able to growth with low inputs in marginal and/or agriculturally degraded lands (Quinn et al. 2015; Tilman et al. 2006). Water deficit stress and salinity are most serious factors limiting the crop productivity. During the onset and development of salt stress within a plant, major biosynthetic processes such as photosynthesis, protein synthesis and lipid metabolism are affected. Plants have evolved a number of mechanisms to deal with excess cations, such as sodium exclusion from their cells and sodium compartmentation (Blumwald 2000; Deinlein et al. 2014). Vacuolar Na^+/H^+ antiporters (NHXs) play significant roles in the removal of excess sodium from the cytoplasm by compartmentalization into the vacuoles (Apse et al. 1999). NHXs activities are regulated by cellular pH and are dependent on tonoplast H^+ fluxes (Bassil et al. 2011b). Two electrogenic vacuolar H^+ pumps, the V-type H^+-ATPase (V-ATPase) and the pyrophosphatase (V-PPiase) generate the electrochemical H^+ gradient that drive the antiporters' activity (Apse and Blumwald 2007). The vacuolar H^+ pumps play paramount roles in growth and development, adjusting their activity and maintaining cellular solute homeostasis under both normal and salinity conditions (Queiros et al. 2009). A relationship between NHXs and V-PPiase, contributing to salt tolerance was suggested (Queiros et al. 2009; Undurraga et al. 2012) and the expression of both *NHX* and *V-PPiase* resulted in a higher tolerance than that achieved by the expression of the individual genes (Bao et al. 2016; Bhaskaran and Savithramma 2011; Zhao et al. 2006). At the tissue level, excess of Na^+ ions can be avoided by the removal of Na^+ from the xylem sap into the surrounding xylem parenchyma cells, thereby decreasing the Na^+ toxicity at the leaves, with the concomitant higher K^+/Na^+ ratio in the xylem and shoots (Deinlein et al. 2014). Class I *HKT8* (OsHKT1;5, AtHKT1;1) transporter, which is mainly Na^+ specific, was shown to play a significant role in the xylem Na^+ removal (Byrt et al. 2007; Davenport et al. 2007; Kobayashi et al. 2017; Plett et al. 2010; Ren et al. 2005; Sunarpi et al. 2005).

Here, we investigated the physiological and molecular responses to salinity of two *B. sylvaticum* natural accessions inhabiting two regions of the world with contrasting climates *(B. sylvaticum* Osl 1, Norway and *B. sylvaticum* Ain 1, Tunisia). Our results indicated that Osl 1 accession displayed higher salt tolerance than Ain 1 and the enhanced salt tolerance was characterized by a better ion homeostasis with higher Na^+ compartmentalization and lower tissue Na^+ allocation.

Results

The responses of Osl1 and Ain1 mature plants to salinity

In order to characterize the effect of salinity on the biomass of both *B. sylvaticum* accessions (Fig. 1a), plants were gradually exposed to 25, 50, 100 and 150 mM NaCl. Salt treatments generally lead to a concentration-dependent inhibition of growth, which was quantified by the relative reduction of the DW of the plant aerial parts, as compared to the non-stressed control. Ain1, but not Osl1, displayed a strong decrease in biomass upon exposure to salt (Fig. 1b). Measurements of the shoot Na^+ and K^+ contents revealed a higher contents of Na^+ and lower contents of K^+ in Ain1 as compared to Osl1 under salinity (Fig. 1c), leading to a higher K^+/Na^+ ratio in Osl1 (Fig. 1c). To estimate whether the differences in biomass were accompanied by physiological and biochemical changes, we measured leaf photosynthesis, transpiration, chlorophyll and protein contents (Fig. 2). Under

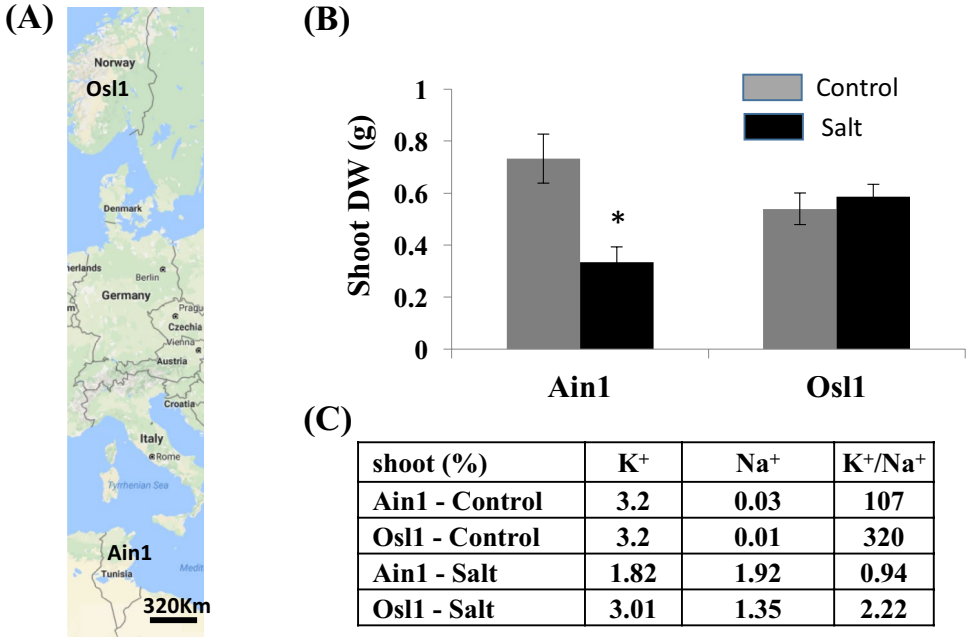

(C)

shoot (%)	K^+	Na^+	K^+/Na^+
Ain1 - Control	3.2	0.03	107
Osl1 - Control	3.2	0.01	320
Ain1 - Salt	1.82	1.92	0.94
Osl1 - Salt	3.01	1.35	2.22

Fig. 1 Effects of salinity on biomass, Na^+ and K^+ contents of two *B. sylvaticum* accessions. **a** Geographical habitat of the *B. sylvaticum* accessions; **b** shoot biomass. Values are the mean ± SE (n = 7–13); **c** shoot Na^+ and K^+ contents. Values represent a bulk of three independent plants. Plants were grown in the presence and absence of 150 mM NaCl. The data were analyzed using Student's *t* test. Asterisks indicate significant differences within a genotype for each treatment ($P \leq 0.05$)

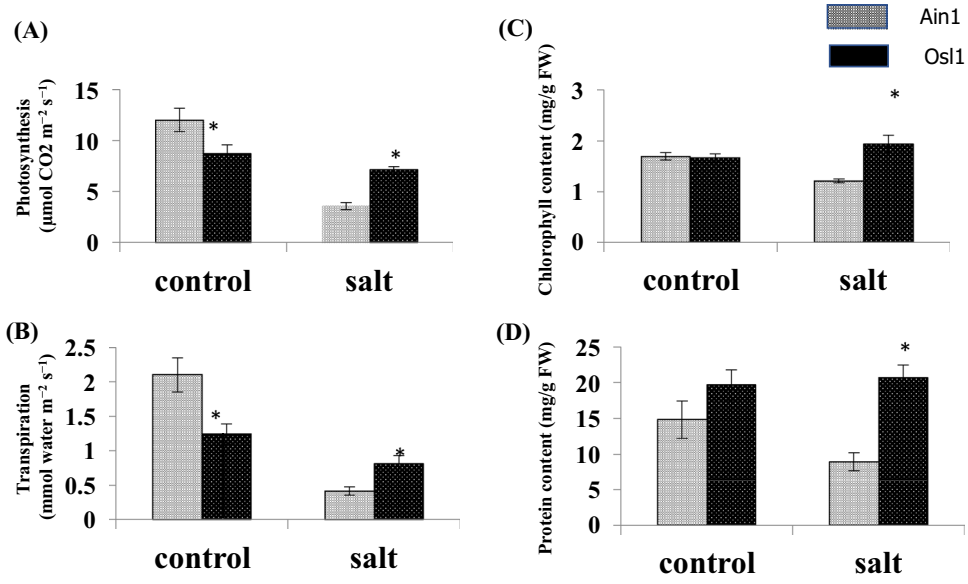

Fig. 2 Effects of salt-stress on shoot parameters of two *B. sylvaticum* accessions. Analysis of **a** photosynthesis, **b** transpiration, **c** chlorophyll and **d** protein content. Values are mean ± SE (n = 3–6). Plants were grown in the presence and absence of 150 mM NaCl. The data were analyzed using Student's *t* test. Asterisks indicate significant differences ($P \leq 0.05$)

normal growth conditions, Osl1 exhibited lower photosynthesis and transpiration than Ain1 (Fig. 2a, b). In contrast, under stress conditions, Osl1 showed higher photosynthesis, transpiration, chlorophyll and protein contents than Ain 1 (Fig. 2a–d). We also quantified changes in the leaf primary metabolites in response to salt (Table S1). Overall, most of the changes detected were showing higher metabolite accumulation in Osl1 than Ain1 with emphasis mostly in amino acids contents. In addition, some metabolites associated with salt stress response (e.g. ornithine, hydroxyproline, arginine, spermidine, 4-hydroxycinnamic acid, sinapic acid) were constitutively higher in Osl1 (Table S1). The expression analysis of genes encoding enzymes associated with proline and polyamine biosynthesis pathways confirmed the metabolomics data (Table S2). When the plants were exposed to 300 mM NaCl for a prolonged period of time, both accessions displayed significant declines in DW, transpiration and photosynthesis (Fig. S1).

Response of shoots and roots to short-term salt stress

We evaluated the response of roots and shoots to short-term salt stress in hydroponically-grown plants exposed to 100 mM NaCl (Fig. 3a). Similar to the response of mature plants to salt, a significant decrease in DW was seen in Ain

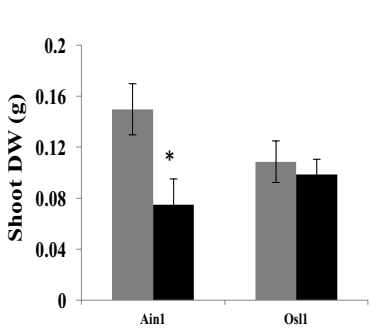

(C)

shoot (%)	K^+	Na^+	K^+/Na^+
Ain1 – salt	1.88± 0.08	1.5 ± 0.06	1.2 ± 0.09
Osl1 – salt	2.4± 0.09 *	0.34 ± 0.06*	7.5 ± 1.1 *
Ain1 – control	3.62± 0.14	0.03 ± 0.003	125 ± 23
Osl1 – control	3.12± 0.05*	0.01*	312 ± 5*

Fig. 3 Effect of salinity on shoot biomass, Na^+ and K^+ content of two *B. sylvaticum* accessions grown hydroponically. **a** Hydroponics system, **b** shoot biomass; **c** shoot Na^+ and K^+. Values are mean ± SE (n = 3–5). Plants were grown hydroponically in the presence of 100 mM NaCl. The data were analyzed using Student's *t* test. Asterisks indicate significant differences within a treatment for each genotype (**b**) or within genotype for each treatment (**c**) ($P \leq 0.05$)

1 plants while no NaCl-induced changes in DW were seen in Osl1 plants (Fig. 3b). In the shoots, both Ain 1 and Osl1 displayed a decrease in K^+ contents, while the increase in Na^+ contents was five times higher in Ain1 shoots (Fig. 3c), leading to a higher K^+/Na^+ in Osl1 shoots. In order to assess whether differences in shoot Na^+ contents were due to a possible difference in the Na^+ permeability of the shoot cells, we isolated shoot protoplasts and quantified Na^+ contents of protoplasts exposed to NaCl using the fluorescent indicator CoroNa Green. Our results indicated that the permeability of the shoot cell plasma membranes to Na^+ was similar in Ain1 and Osl1 (Fig. S2). The exclusion of Na^+ from leaf blades has been shown to be mediated by the action of HKT-type of transporters that mediate the unloading of Na^+ from the xylem, a process where Na^+ ions are retrieved from the apoplastic space resulting in a reduced transfer of Na^+ into the xylem vessels (Horie et al. 2009; Kobayashi et al. 2017). We tested whether differences in the Na^+ transport from roots to shoots led to the lower shoot Na^+ contents of Osl1, by measuring xylem Na^+ and K^+ contents of de-topped plants. Osl1 xylem contained lower Na^+ and higher K^+ than Ain1, leading to higher K^+/Na^+ ratio than Ain1 (Fig. 4). The differences in root to shoot Na^+ transport were highly correlated with the expression levels of *BsHKT8* and *BsSOS1* in both, root and shoot (Fig. 5f, g and Fig. S3).

We characterized the root response of both accessions to salt stress. Interestingly, the quantification of Na^+ contents in the root revealed that in contrast with shoot tissues (Fig. 3c), under salinity, Osl1 roots contained higher amounts of Na^+ than Ain1 (Fig. 5a), suggesting increased root vacuolar Na^+ compartmentation. Given the role of NHX-type antiporters in vacuolar sodium accumulation (Blumwald 2000), we assessed the expression of the most abundant vacuolar *NHX1* and *NHX2* (Bassil et al. 2011b). Both *BsNHX1* and *BsNHX2* root expression was higher in Osl1 than in Ain1 (Fig. 5b, c). Since the vacuolar cation/proton exchange is energized by the operation of vacuolar H^+ translocating enzymes (V-ATPase and V-PPiase); (Rea and Sanders 1987; Queiros et al. 2009), we evaluated the expression and protein levels of V-PPase (BsAVP1) in Osl1 and Ain1 exposed

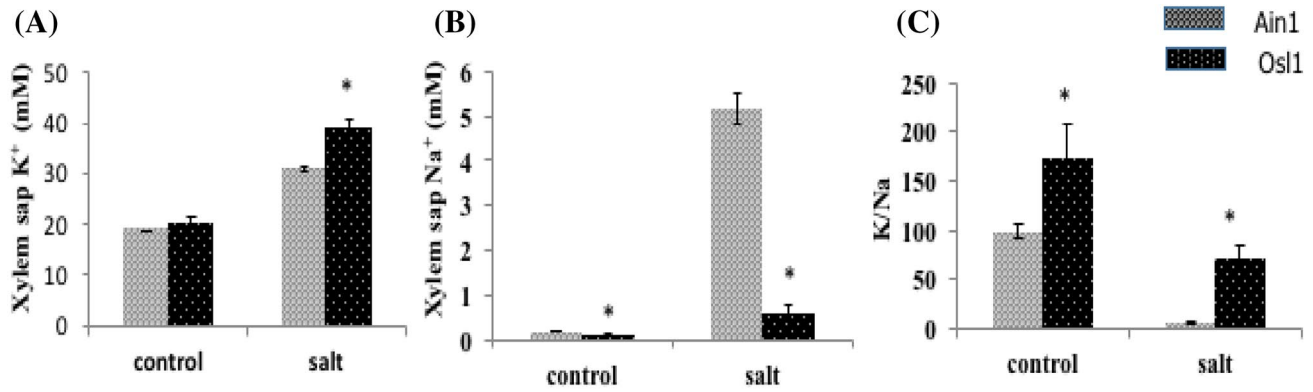

Fig. 4 Cation concentrations in the xylem sap of Ain1 and Osl1 in response to salinity. **a** K^+; **b** Na^+ and **c** K^+/Na^+ ratio. Values are the mean ± SE (n = 3–5). Data were analyzed using Student's *t* test. Asterisks indicate significant differences ($P \leq 0.05$)

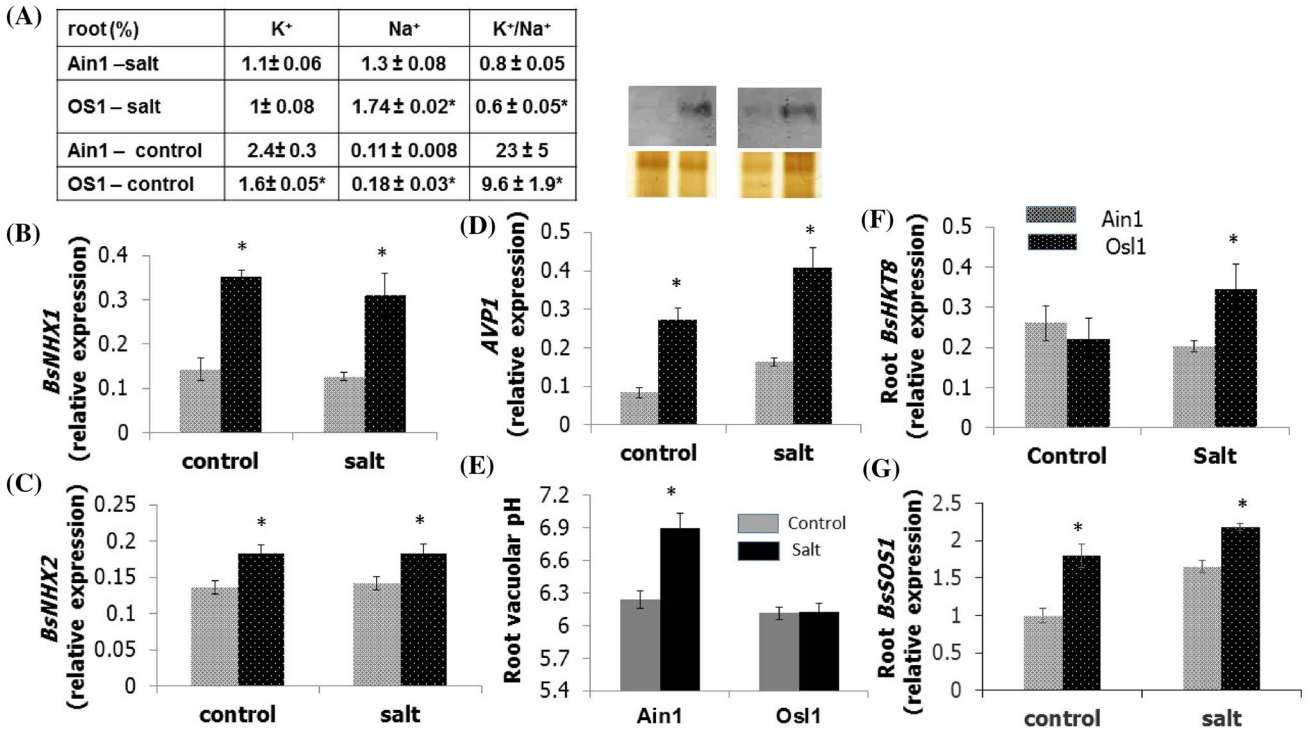

Fig. 5 Effects of salinity on root Na^+ and K^+ contents of Ain1 and Osl1, expression of root *BsNHXs, BsAVP1, BsHKT8, BsSOS1* and root vacuolar pH. **a** Root Na^+ and K^+ contents; **b–d** qRT-PCR expression analysis of **b** *BsNHX1*, **c** *BsNHX2* and **d** *BsAVP1* and protein abundance in roots under control and salinity conditions. Silver stained PAGE of microsomal pellets isolated from Ain1 and Osl1 grown in the presence and absence of 100 mM NaCl (lower panel). Anti-AVP1 (81 kDa) western blots of PAGE of microsomal pellets isolated from Ain1 and Osl1 grown in the presence and absence of 100 mM NaCl (upper panel). **e** Root vacuolar pH of seedlings grown in the presence and absence of 50 mM NaCl. **f, g** qRT-PCR analysis of **f** *BsHKT8* and **g** *BsSOS1*. Values are the mean ± SE (n = 3–4). Data were analyzed using Student's *t* test. Asterisks indicate significant differences within a treatment for each genotype (**a–d, f, g**) or within genotype for each treatment (**e**) ($P \leq 0.05$)

to salinity. *BsAVP1* expression and protein abundance was higher in Osl1 than in Ain1 roots (Fig. 5d) and it increased in both accessions during the exposure of the plants to NaCl, although the expression and protein abundance remained higher in Osl1 roots and leaves (Fig. 5d, Fig. S3). Using the fluorescent dye BCECF, we measured the vacuolar pH in root cells of Osl1 and Ain1 (Fig. 5e). Under control conditions, the vacuolar pH of both accessions was similar. Salinity induced the alkalinization of Ain1 root vacuoles while the pH in Ain1 vacuoles remained constant (Fig. 5e).

Discussion

Here, we characterized the responses of two *B. sylvaticum* accessions, isolated from two geographical areas with contrasting climates (i.e. Osl1 from Norway and Ain1 from Tunisia). Our aim was to characterize stress tolerance mechanism(s) in this model perennial grass specie that could contribute to shed light on similar mechanisms in leading candidates for dedicated biomass crops such as switchgrass and *Miscanthus* (Carroll and Somerville 2009; Dohleman and Long 2009). When exposed to salinity, Osl1 plants displayed higher tolerance to salinity than the Ain1 accession, as indicated by increased growth, higher photosynthesis, protein and chlorophyll contents. Notably, Osl1 protein and chlorophyll contents were not affected by the stress treatment. These results were consistent with the reported response of plants to mild stress conditions (Aghaleh et al. 2009; Ayala-Astorga and Alcaraz-Meléndez 2010). Interestingly, transpiration and photosynthesis were lower in Osl1 than in Ain1 grown under well-watered conditions. Since photosynthesis is positively correlated with biomass accumulation, these physiological differences might explain some of the morphological differences between the two species (e.g. Ain1 displayed bigger size than Osl1 when grown under low salinity), (Steinwand et al. 2013). We also analyzed the overall metabolic response to salinity of leaves from both accessions. Osl1 displayed higher amounts of Ornithine and Proline, amino acids known as osmoprotectans (Kaur and Asthir 2015), polyamines (e.g. Ornithine, Spermidine) (Kaur and Asthir 2015; Liu et al. 2015;

Vogt 2010) and phenylpropanoids (e.g. Sinapic Acid) (Vogt 2010). This response indicated significant roles of osmotic adjustment and polyamine synthesis in Osl1 shoots under mild stress conditions, as shown by the increased expression of delta-1-pyrroline-5-carboxylate synthetase (*P5CS*) and Spermine synthase (*SMS*) encoding enzymes associated with the synthesis of proline and polyamines, respectively. Interestingly, when the two accessions were grown for prolonged periods of time in the presence of 300 mM NaCl, their growth was severely inhibited and did not display any differential response, indicating that Osl1 is only tolerant to moderate salinity. The analysis of xylem sap, obtained from plants grown in the presence of NaCl revealed that Osl1 maintained lower Na^+ contents than Ain1 and a higher K^+/Na^+ ratio. Although many salt tolerant plant species displayed a relatively lower permeability to Na^+ (Volkov 2015), shoot protoplasts from both Osl1 and Ain1 displayed similar membrane permeability to Na^+. Moreover, analysis of root ion contents revealed that Osl1 roots contained higher Na^+ than Ain1 roots. These results suggested that the increased tolerance displayed by Osl1 plants was associated with two mechanisms for Na^+ homeostasis; the maintenance of elevated Na^+ concentrations, albeit not deleterious, in the root cells and the exclusion of Na^+ ions from the xylem that limited the amount of Na^+ reaching the shoots.

The compartmentation of Na^+ in the root vacuoles was indicated by the increased expression of the more abundant vacuolar Na^+/H^+ antiporters *BsNHX1* and *BsNHX2* and by the increased expression of the *BsV-PPiase* and higher BsV-PPiase protein content of Osl1. Interestingly, although NHXs expression was constitutively higher in Osl1 than in Ain1, NHXs expression remained unchanged during salt treatments in both accessions (Fig. 5a, b). Mechanism(s) of post-translational regulation regulating the NHXs activity might take place under salt treatments. Yamaguchi et al. (2005) showed that the AtNHX1 activity was regulated by the interaction of the antiporter with AtCaM15, a Calmodulin isoform, and that this interaction was dependent on the vacuolar pH (Yamaguchi et al. 2005). The salt-dependent alkalinization of the root vacuolar pH in Ain 1, but not in Osl1, correlated well with the reported salinity-induced vacuolar alkalinization (Gruwel et al. 2001; Katsuhara et al. 1989). The increased V-PPiase in the Osl1 root vacuoles, contributed to maintain the relatively lower vacuolar pH in the Osl1 roots and energized the vacuolar BsNHXs, contributing to the increased Na^+ compartmentation in the root vacuoles. In addition to the role of vacuolar Na^+ compartmentation in plant tolerance to salinity, the exclusion of Na^+ ions from the xylem through the activity of the HKT-type transporters has been shown to be an important mechanism contributing to the salt tolerance of many plant species (Deinlein et al. 2014; Byrt et al. 2007; Davenport et al. 2007; Kobayashi et al. 2017; Plett et al. 2010; Ren et al. 2005; Sunarpi et al. 2005). The higher expression of *BsHKT8* and *BsSOS1* supported the notion of lower Na^+ concentrations and the high K^+/Na^+ ratio in the shoots of Osl1. Interestingly, in Osl1, the expression of *BsHKT8* was higher in roots than in leaves (Fig S3), emphasizing the essential role of *BsHKT8* in the regulation of the unloading of Na^+ ions from the xylem to the xylem parenchyma, limiting the amounts of Na^+ translocating from the roots to the shoots. Our results further highlight the role of Na^+ transport systems in plant salt tolerance. The concerted action of NHX-type transporters, compartmentalizing Na^+ in the vacuoles, SOS1-type antiporters further decreasing cytosolic Na^+ and HKT-type transporters reducing the Na^+ concentrations exported to the leaves, contributed to diminishing the deleterious effects on photosynthesis (Deinlein et al. 2014). The relationship between Osl1 salt tolerance and its natural growth environment (i.e. Norway) is not yet clear and need further investigation. However, some of the salt tolerance mechanism(s) described here (i.e. ion homeostasis and leaf osmotic adjustment) might contribute to the extreme freezing tolerance of Osl1 (Sade et al. unpublished results).

Materials and methods

Plant material and growth conditions

Seeds from *B. sylvaticum* Ain1 and Osl1 accessions were obtained from the USDA National Plant Germplasm System. Ain1 and Osl1 seeds were germinated on moist germination paper for 14 days at 24 °C 16-h/8-h day/night and 24 °C/18 °C and 150 µmol m^{-2} s^{-1} light intensity. For greenhouse experiments, seedlings were transplanted into 1-L pots filled with moist agronomy mix (equal parts of redwood compost, sand and peat moss) and fertilized with a nutrient solution containing: N 77 ppm, P 20 ppm, K 75 ppm, Ca 27 ppm, Mg 17 ppm, S 65 ppm, Fe 1.50 ppm, Mn 0.50 ppm, Zn 0.05 ppm, Mo 0.01 ppm, Cu 0.02 ppm and pH 5.6. Greenhouse conditions were kept at 16-h/8-h day/night and 24 °C/18 °C. Salt stress was imposed at week 4 by 25, 50, 100 and 150 mM NaCl, incrementing weekly. Leaf samples were collected before harvesting. For experiments with high salinity, salt stress was imposed at week 4 by gradually adding solutions supplemented with 25, 50, 100 mM of NaCl for 1 week followed by 150 mM for 3 weeks and 300 mM of NaCl for 1 week. For hydroponics experiments, seedlings were placed into plastic containers, filled with fertilized solution (as described above) and air was bubbled constantly into the containers using air pumps. At 4 weeks, plants were treated with 100 mM NaCl for 3 days and harvested. Root vacuoles and shoot protoplasts were extracted from 2 week-old seedlings grown on moist

germination paper at 16-h/8-h day/night and 24 °C/18 °C 150 µmol m^{-2} s^{-1} light intensity.

Gas-exchange measurements

The measurements of photosynthesis were recorded in plants using a Li-6400 portable gas-exchange system (LI-COR). Photosynthesis was induced by saturating light (1200 µmol m^{-2} s^{-1}) with 400 µmol mol^{-1} CO_2 surrounding the leaf (C_a). The amount of blue light was set to 10% photosynthetically active photon flux density to optimize stomatal aperture. Temperature was set to 25 °C.

Protein quantification

The Bradford (1976) assay was used for protein quantification using bovine serum albumin as a standard.

Quantitative PCR analysis

RNA was extracted from tissue of Ain1 and Osl1 plants grown under well-watered and salt stress conditions. First-strand complementary DNA synthesis, primer design, and quantitative PCR were performed as described before (Peleg et al. 2011). The genes IDs, sequences and the different sets of primers used for the amplification of the different target genes are listed in Table S3. Analysis of the gene expression was calibrated relative to the endogenous *Brachypodium* gene Ubiquitin-conjugating enzyme 18 (Hong et al. 2008).

Chlorophyll measurements

For chlorophyll measurements, the leaves were weighed and ground in liquid N_2. Chlorophyll was extracted in 80% acetone, and the absorbance at 663 and 645 nm was measured using spectrophotometry (Synergy™ Mx Microplate Reader; BioTek, USA). Total chlorophyll contents were calculated as described elsewhere (Porra 2002).

Xylem sap collection and analysis

Plants grown hydroponically were treated with or without 25 mM NaCl for 24 h (higher NaCl concentrations did not yield sufficient sap for analysis). After 24 h, shoots were carefully excised 1 cm above the crown and the roots were left to freely exudate for 5 min followed by carefully cleaning with Kim wipes. Exudates, were then collected for 1 h for all plants and were kept in ice. Twenty µL of xylem sap samples were sent for digestion and analysis at the Interdisciplinary Center for Plasma Mass Spectrometry at the University of California at Davis (http://www.ICPMS.UCDavis.edu) using an Agilent 7500ce ICP-MS (Agilent Technologies, Palo Alto, CA). Samples, a method blank, and digestion quality control standards were digested by adding 30 µL concentrated Trace Metals Grade HNO_3 (Fisher Scientific) at room temperature and allowing the samples to react for 1 h. The samples were then transferred to 2.0 mL microcentrifuge tubes using 50 µL 18.2 MΩ-cm water, and introduced to a hot block that was ramped up to 95 °C over approximately 1 h. The samples were allowed to cool and then, brought to a final volume of 1 mL with 18.2 MΩ-cm water prior to analysis.

Immunoblot analyses

Plant tissues were frozen in liquid N_2 and grinded in extraction buffer [HEPES 50 mM; NaCl 100 mM; KCl 10 mM; 0, 4 M sucrose; PMSF 1 mM; Protease inhibitor 1% (v/v)] followed by 20,000×*g* for 10 min. Supernatants were collected and a 2nd centrifugation was done at 126,000×*g* for 45 min. Supernatants were discarded and pellets were resuspended in extraction buffer + 1% TX-100 and incubated for 30 min at 4 °C under constant shaking, followed by a 3rd centrifugation at 88,000×*g* for 45 min. Supernatants were collected and contained the microsomal proteins.Proteins (10–20 µg) were separated by SDS-PAGE, transferred to a polyvinylidene difluoride membrane (Bio-Rad, Hercules, CA), and probed as described previously (Wang et al. 2011). Antibody (dilution 1:1000 in 5% blotting grade blocker; Bio-Rad, Hercules, CA) raised against AVP1 were a kind gift from Dr. Phil A. Rea, University of Philadelphia. Horseradish peroxidase-conjugated secondary antibodies were purchased from Santa Cruz Biotechnology (Dallas, TX). Silver staining was done as described (Chevallet et al. 2006).

Measurement of Na^+ in isolated protoplasts

Protoplasts were isolated from 0.3 g shoots of 16 days-old plants grown on moist germination paper. The enzyme solution contained 1% cellulase (w/v) (Onozuka R-10), 1.33% macerozyme R-10, 0.1% bovine serum albumin, 1 mM $CaCl_2$, 10 mM KCl and 10 mM MES/KOH, pH 5.7. The osmolality of the enzyme solution was adjusted to 300 mOsmol kg^{-1} using D-sorbitol. Shoots were cut and pieces were incubated in 15 mL enzyme solution at 25 °C for 6 h with gently shaking. The released protoplasts were filtered through Miracloth (Millipore, Billerica, MA) and diluted with two volumes of buffer containing 2 mM $CaCl_2$, 1 mM $MgCl_2$, 5 mM KCl, 10 mM Sucrose, and 10 mM MES/KOH buffer pH 5.7 (osmolality, 400 mOsmol kg^{-1}). The diluted protoplasts were centrifuged for 12 min at 400 g at 4 °C. The pellets, containing the protoplasts were resuspended in 1.2 mL containing: 4 mM KCl, 0.1 mM $CaCl_2$, 1 mM $MgCl_2$, and 10 mMMES/KOH, pH 5.7. The osmolality of the suspension buffer was adjusted to 400 mOsmol kg^{-1} using D-sorbitol. The protoplast suspension was stored on

ice and aliquots used for sodium dye recording. CoroNa™ Green, AM (Molecular Probes, Invitrogen, Carlsbad, CA) at 10 µM was loaded into *B. sylvaticum* protoplasts suspended in dye loading buffer. Dye loading was carried out in the dark at 37 °C for 30 min in the presence of 600 µM Eserine. Unincorporated dye was washed off with 2 mM $CaCl_2$, 1 mM $MgCl_2$, 5 mM KCl, 10 mM Sucrose, and 10 mM MES/KOH buffer (osmolality, 400 mOsmol kg^{-1}, pH 5.7) and the dye loaded protoplasts were re-suspended in the same buffer. Twenty µL dye-loaded protoplasts were settled on coverslips coated with poly-D-lysine for microscopy. Dye fluorescence images were collected using a Leica DMRE microscope equipped with a ×20 objective after excitation with 488 nm wavelength. CoroNa™ Green intensities were determined before and after 3 min exposure to various NaCl concentration in individual protoplasts with ImageJ (http://imagej.nih.gov/ij/download/). A curve representing *B. sylvaticum* protoplast response to different concertation of NaCl in the presence of the dye is shown in Fig. S5.

Primary metabolite profiling by gas chromatography–mass spectrometry

Metabolites were extracted from 8 week-old leaves as described by Giavalisco et al. (2011). Vacuum-dried polar phase samples (150 µL) were derivatized and subjected to GC–MS analysis as described by Lisec et al. (2015). The GC–MS data were obtained using an Agilent 7683 series auto-sample (Agilent Technologies, http://www.home.agilent.com), coupled to an Agilent 6890 gas-chromatograph–Leco Pegasus two time-of-flight mass spectrometer (Leco; http://www.leco.com/). Chromatogram acquisition parameters were as described previously (Caldana et al. 2011). Chromatograms were exported from LECO CHROMATOF software (version 3.34) to R software. Ion extraction, peak detection, retention time alignment and library searching were obtained using the TargetSearch package from Bioconductor (Cuadros-Inostroza et al. 2009); the resulting data matrix was used for further analysis.

Measurement of vacuolar pH

Vacuolar pH from root cells was measured using the pH-sensitive dye BCECF-AM as previously described (Bassil et al. 2011a, 2013; Krebs et al. 2010). Briefly, 10 day-old seedlings were grown on moist germination paper with or without 50 mM NaCl for 36 h. For dye loading, seedlings were incubated in 10 µM BCECF-AM with 0.02% pluronic F-127 (Molecular Probes, Carlsbad, CA) in water for 1 h in darkness at 22 °C, and washed twice before imaging. Fluorescence images were collected using a Leica DMRE equipped with a ×20 objective, running Metamorph v7.7 (Molecular Devices, Sunnyvale CA) and a Sutter Lamda2 filter wheel control (Sutter Instruments, Novato CA). Single emission between 525 and 550 nm was collected after sequential excitation with 458 and 488 nm. After background correction, the integrated pixel intensity was measured for both the 458 and 488 nm-excited images, and ratios were calculated using ImageJ (http://imagej.nih.gov/ij/download/). Fluorescence ratio values were used to calculate the pH from a calibration curve generated by imaging seedlings that were equilibrated 15 min before observation in buffer containing 50 mM BTP-HEPES or (pH 5.0–7.4) and 50 mM ammonium acetate.

Tissue Na^+ and K^+ contents

Roots and shoots were harvested and oven dried for 3 days at 70 °C. Tissue was scaled, grinded, digested with nitric acid and hydrogen peroxide as described by Sah and Miller (1992) and analyzed using Inductively Coupled Plasma Atomic Emission Spectrometry (ICP¬AES).

Statistical analysis

The JMP statistical package (SAS Institute) was used for statistical analyses. The experiments were based on a complete randomized design.

Acknowledgements This research was supported grants from United States Department of Energy Number #DE-SC0008797 and #DE-AC02-05CH11231. XK was supported by a scholarship from the China Scholarship Council (CSC) and Nanjing Agricultural University.

Author contributions NS, MRW, and EdB provided research ideas and designed the experiments. NS, MRW, XK, YB, MW, IK, WDS, JPV, CMT, RT and EB participated in the implementation of the experiment, sample collection, and laboratory analysis. NS and EdB wrote the paper.

References

Aghaleh M, Niknam V, Ebrahimzadeh H, Razavi K (2009) Salt stress effects on growth, pigments, proteins and lipid peroxidation in *Salicornia persica* and *S. europaea*. Biol Plant 53:243–248. https://doi.org/10.1007/s10535-009-0046-7

Apse MP, Blumwald E (2007) Na^+ transport in plants. Febs Lett 581(12):2247–2254. https://doi.org/10.1016/j.febslet.2007.04.014

Apse MP, Aharon GS, Snedden WA, Blumwald E (1999) Salt tolerance conferred by overexpression of a vacuolar Na^+/H^+ antiport in Arabidopsis. Science 285(5431):1256–1258. https://doi.org/10.1126/science.285.5431.1256

Ayala-Astorga G, Alcaraz-Meléndez L (2010) Salinity effects on protein content, lipid peroxidation, pigments, and proline in *Paulownia imperialis* (Siebold & Zuccarini) and *Paulownia fortunei* (Seemann & Hemsley) grown in vitro. Electron J Biotechnol. https://doi.org/10.2225/vol13-issue5-fulltext-13

Bao AK, Du BQ, Touil L, Kang P, Wang QL, Wang SM (2016) Co-expression of tonoplast cation/H^+ antiporter and H^+-pyrophosphatase from xerophyte *Zygophyllum xanthoxylum* improves alfalfa plant growth under salinity, drought and

field conditions. Plant Biotechnol J 14(3):964–975. https://doi.org/10.1111/pbi.12451

Bassil E, Tajima H, Liang YC, Ohto M, Ushijima K, Nakano R, Esumi T, Coku A, Belmonte M, Blumwald E (2011a) The Arabidopsis Na(+)/H(+) antiporters NHX1 and NHX2 control vacuolar pH and K(+) homeostasis to regulate growth, flower development, and reproduction. Plant Cell 23(9):3482–3497. https://doi.org/10.1105/tpc.111.089581

Bassil E, Tajima H, Liang YC, Ohto M, Ushijima K, Nakano R, Esumi T, Coku A, Belmonte M, Blumwald E (2011b) The Arabidopsis Na^+/H^+ antiporters NHX1 and NHX2 control vacuolar pH and K^+ homeostasis to regulate growth, flower development, and reproduction. Plant Cell 23(9):3482–3497. https://doi.org/10.1105/tpc.111.089581

Bassil E, Krebs M, Halperin S, Schumacher K, Blumwald E (2013) Fluorescent dye based measurement of vacuolar pH and K^+. Bio-Protocol. https://doi.org/10.21769/BioProtoc.810. http://www.bio-protocol.org/e810

Bhaskaran S, Savithramma DL (2011) Co-expression of *Pennisetum glaucum* vacuolar Na^+/H^+ antiporter and Arabidopsis H^+-pyrophosphatase enhances salt tolerance in transgenic tomato. J Exp Bot 62(15):5561–5570. https://doi.org/10.1093/jxb/err237

Blumwald E (2000) Sodium transport and salt tolerance in plants. Curr Opin Cell Biol 12(4):431–434. https://doi.org/10.1016/s0955-0674(00)00112-5

Bradford MM (1976) Rapid and sensitive method for quantitation of microgram quantities of protein utilizing principle of protein-dye binding. Anal Biochem 72(1–2):248–254. https://doi.org/10.1006/abio.1976.9999

Brkljacic J, Grotewold E, Scholl R, Mockler T, Garvin DF, Vain P, Brutnell T, Sibout R, Bevan M, Budak H, Caicedo AL, Gao CX, Gu Y, Hazen SP, Holt BF, Hong SY, Jordan M, Manzaneda AJ, Mitchell-Olds T, Mochida K, Mur LAJ, Park CM, Sedbrook J, Watt M, Zheng SJ, Vogel JP (2011) *Brachypodium* as a model for the grasses: today and the future. Plant Physiol 157(1):3–13. https://doi.org/10.1104/pp.111.179531

Byrt CS, Platten JD, Spielmeyer W, James RA, Lagudah ES, Dennis ES, Tester M, Munns R (2007) HKT1;5-like cation transporters linked to Na^+ exclusion loci in wheat, Nax2 and Kna1. Plant Physiol 143(4):1918–1928. https://doi.org/10.1104/pp.093476

Caldana C, Degenkolbe T, Cuadros-Inostroza A, Klie S, Sulpice R, Leisse A, Steinhauser D, Fernie AR, Willmitzer L, Hannah MA (2011) High-density kinetic analysis of the metabolomic and transcriptomic response of Arabidopsis to eight environmental conditions. Plant J 67(5):869–884. https://doi.org/10.1111/j.1365-313X.2011.04640.x

Carroll A, Somerville C (2009) Cellulosic biofuels. Annu Rev Plant Biol 60:165–182. https://doi.org/10.1146/annurev.arplant.043008.092125

Chevallet M, Luche S, Rabilloud T (2006) Silver staining of proteins in polyacrylamide gels. Nat Protoc 1(4):1852–1858. https://doi.org/10.1038/nprot.2006.288

Cuadros-Inostroza A, Caldana C, Redestig H, Kusano M, Lisec J, Pena-Cortes H, Willmitzer L, Hannah MA (2009) TargetSearch: a bioconductor package for the efficient preprocessing of GC-MS metabolite profiling data. BMC Bioinform. https://doi.org/10.1186/1471-2105-10-428

Davenport RJ, Munoz-Mayor A, Jha D, Essah PA, Rus A, Tester M (2007) The Na^+ transporter AtHKT1;1 controls retrieval of Na^+ from the xylem in Arabidopsis. Plant Cell Environ 30(4):497–507. https://doi.org/10.1111/j.1365-3040.2007.01637.x

Deinlein U, Stephan AB, Horie T, Luo W, Xu GH, Schroeder JI (2014) Plant salt-tolerance mechanisms. Trends Plant Sci 19(6):371–379. https://doi.org/10.1016/j.tplants.2014.02.001

Dohleman FG, Long SP (2009) More productive than maize in the midwest: how does *Miscanthus* do it? Plant Physiol 150(4):2104–2115. https://doi.org/10.1104/pp.109.139162

Giavalisco P, Li Y, Matthes A, Eckhardt A, Hubberten HM, Hesse H, Segu S, Hummel J, Kohl K, Willmitzer L (2011) Elemental formula annotation of polar and lipophilic metabolites using C-13, N-15 and S-34 isotope labelling, in combination with high-resolution mass spectrometry. Plant J 68(2):364–376. https://doi.org/10.1111/j.1365-313X.2011.04682.x

Glover JD, Reganold JP (2010) Perennial grains food security for the future. Issues Sci Technol 26(2):41–47

Glover JD, Reganold JP, Bell LW, Borevitz J, Brummer EC, Buckler ES, Cox CM, Cox TS, Crews TE, Culman SW, DeHaan LR, Eriksson D, Gill BS, Holland J, Hu F, Hulke BS, Ibrahim AMH, Jackson W, Jones SS, Murray SC, Paterson AH, Ploschuk E, Sacks EJ, Snapp S, Tao D, Van Tassel DL, Wade LJ, Wyse DL, Xu Y (2010) Increased food and ecosystem security via perennial grains. Science 328(5986):1638–1639. https://doi.org/10.1126/science.1188761

Gordon SP, Liu L, Vogel JP (2016) The genus *Brachypodium* as a model for perenniality and polyploidy. In: Vogel JP (ed) Genetics and genomics of *Brachypodium*. Springer, Cham, pp 313–325

Gruwel MLH, Rauw VL, Loewen M, Abrams SR (2001) Effects of sodium chloride on plant cells; a P-31 and Na-23 NMR system to study salt tolerance. Plant Sci 160(5):785–794. https://doi.org/10.1016/s0168-9452(00)00424-6

Hong SY, Seo PJ, Yang MS, Xiang F, Park CM (2008) Exploring valid reference genes for gene expression studies in Brachypodium distachyon by real-time PCR. BMC Plant Biol. https://doi.org/10.1186/1471-2229-8-112

Horie T, Hauser F, Schroeder JI (2009) HKT transporter-mediated salinity resistance mechanisms in Arabidopsis and monocot crop plants. Trends Plant Sci 14(12):660–668. https://doi.org/10.1016/j.tplants.2009.08.009

Katsuhara M, Kuchitsu K, Takeshige K, Tazawa M (1989) Salt stress-induced cytoplasmic acidification and vacuolar alkalization in nitellopsis-obtusa cells: in vivo p-31-nuclear magnetic-resonance study. Plant Physiol 90(3):1102–1107. https://doi.org/10.1104/pp.90.3.1102

Kaur G, Asthir B (2015) Proline: a key player in plant abiotic stress tolerance. Biol Plant 59(4):609–619. https://doi.org/10.1007/s10535-015-0549-3

Kobayashi NI, Yamaji N, Yamamoto H, Okubo K, Ueno H, Costa A, Tanoi K, Matsumura H, Fujii-Kashino M, Horiuchi T, Al Nayef M, Shabala S, An G, Ma JF, Horie T (2017) OsHKT1;5 mediates Na^+ exclusion in the vasculature to protect leaf blades and reproductive tissues from salt toxicity in rice. Plant J 91(4):657–670. https://doi.org/10.1111/tpj.13595

Krebs M, Beyhl D, Gorlich E, Al-Rasheid KAS, Marten I, Stierhof YD, Hedrich R, Schumacher K (2010) Arabidopsis V-ATPase activity at the tonoplast is required for efficient nutrient storage but not for sodium accumulation. PNAS 107(7):3251–3256. https://doi.org/10.1073/pnas.0913035107

Lisec J, Schauer N, Kopka J, Willmitzer L, Fernie AR (2015) Gas chromatography mass spectrometry-based metabolite profiling in plants (vol 1, pg 387, 2006). Nat Protoc 10(9):1457–1457. https://doi.org/10.1038/nprot0915-1457a

Liu JH, Wang W, Wu H, Gong XQ, Moriguchi T (2015) Polyamines function in stress tolerance: from synthesis to regulation. Front Plant Sci. https://doi.org/10.3389/fpls.2015.00827

Lu F, Lipka AE, Glaubitz J, Elshire R, Cherney JH, Casler MD, Buckler ES, Costich DE (2013) Switchgrass genomic diversity, ploidy, and evolution: novel insights from a network-based SNP discovery protocol. PLoS Genet. https://doi.org/10.1371/journal.pgen.1003215

McLaughlin SB, Kszos LA (2005) Development of switchgrass (*Panicum virgatum*) as a bioenergy feedstock in the United States. Biomass Bioenergy 28(6):515–535. https://doi.org/10.1016/j.biombioe.2004.05.006

Peleg Z, Reguera M, Tumimbang E, Walia H, Blumwald E (2011) Cytokinin-mediated source/sink modifications improve drought tolerance and increase grain yield in rice under water-stress. Plant Biotechnol J 9(7):747–758. https://doi.org/10.1111/j.1467-7652.2010.00584.x

Plett D, Safwat G, Gilliham M, Moller IS, Roy S, Shirley N, Jacobs A, Johnson A, Tester M (2010) Improved salinity tolerance of rice through cell type-specific expression of AtHKT1;1. PLoS ONE. https://doi.org/10.1371/journal.pone.0012571

Porra RJ (2002) The chequered history of the development and use of simultaneous equations for the accurate determination of chlorophylls a and b. Photosyn Res 73(1–3):149–156. https://doi.org/10.1023/a:1020470224740

Queiros F, Fontes N, Silva P, Almeida D, Maeshima M, Geros H, Fidalgo F (2009) Activity of tonoplast proton pumps and Na^+/H^+ exchange in potato cell cultures is modulated by salt. J Exp Bot 60(4):1363–1374. https://doi.org/10.1093/jxb/erp011

Quinn LD, Straker KC, Guo J, Kim S, Thapa S, Kling G, Lee DK, Voigt TB (2015) Stress-tolerant feedstocks for sustainable bioenergy production on marginal land. Bioenergy Res 8(3):1081–1100. https://doi.org/10.1007/s12155-014-9557-y

Rea PA, Sanders D (1987) Tonoplast energization: 2 h + pumps, one membrane. Physiol Plant 71(1):131–141. https://doi.org/10.1111/j.1399-3054.1987.tb04630.x

Ren ZH, Gao JP, Li LG, Cai XL, Huang W, Chao DY, Zhu MZ, Wang ZY, Luan S, Lin HX (2005) A rice quantitative trait locus for salt tolerance encodes a sodium transporter. Nat Genet 37(10):1141–1146. https://doi.org/10.1038/ng1643

Sah RN, Miller RO (1992) Spontaneous reaction for acid dissolution of biological tissues in closed vessels. Anal Chem 64(2):230–233. https://doi.org/10.1021/ac00026a026

Steinwand MA, Young HA, Bragg JN, Tobias CM, Vogel JP (2013) *Brachypodium sylvaticum*, a model for perennial grasses: transformation and inbred line development. PLoS ONE. https://doi.org/10.1371/journal.pone.0075180

Sunarpi, Horie T, Motoda J, Kubo M, Yang H, Yoda K, Horie R, Chan WY, Leung HY, Hattori K, Konomi M, Osumi M, Yamagami M, Schroeder JI, Uozumi N (2005) Enhanced salt tolerance mediated by AtHKT1 transporter-induced Na^+ unloading from xylem vessels to xylem parenchyma cells. Plant J 44(6):928–938. https://doi.org/10.1111/j.1365-313X.2005.02595.x

Tilman D, Hill J, Lehman C (2006) Carbon-negative biofuels from low-input high-diversity grassland biomass. Science 314(5805):1598–1600. https://doi.org/10.1126/science.1133306

Undurraga SF, Santos MP, Paez-Valencia J, Yang HB, Hepler PK, Facanha AR, Hirschi KD, Gaxiola RA (2012) Arabidopsis sodium dependent and independent phenotypes triggered by H^+-PPase up-regulation are SOS1 dependent. Plant Sci 183:96–105. https://doi.org/10.1016/j.plantsci.2011.11.011

Vogt T (2010) Phenylpropanoid biosynthesis. Mol Plant 3(1):2–20. https://doi.org/10.1093/mp/ssp106

Volkov V (2015) Salinity tolerance in plants. Quantitative approach to ion transport starting from halophytes and stepping to genetic and protein engineering for manipulating ion fluxes. Front Plant Sci. https://doi.org/10.3389/fpls.2015.00873

Wang SH, Kurepa J, Hashimoto T, Smalle JA (2011) Salt stress-induced disassembly of arabidopsis cortical microtubule arrays involves 26S proteasome-dependent degradation of SPIRAL1. Plant Cell 23(9):3412–3427. https://doi.org/10.1105/tpc.111.089920

Yamaguchi T, Aharon GS, Sottosanto JB, Blumwald E (2005) Vacuolar Na^+/H^+ antiporter cation selectivity is regulated by calmodulin from within the vacuole in a Ca^{2+}- and pH-dependent manner. Proc Natl Acad Sci USA 102(44):16107–16112. https://doi.org/10.1073/pnas.0504437102

Yan J, Chen WL, Luo F, Ma HZ, Meng AP, Li XW, Zhu M, Li SS, Zhou HF, Zhu WX, Han B, Ge S, Li JQ, Sang T (2012) Variability and adaptability of *Miscanthus* species evaluated for energy crop domestication. GCB Bioenergy 4(1):49–60. https://doi.org/10.1111/j.1757-1707.2011.01108.x

Zhao FY, Zhang XJ, Li PH, Zhao YX, Zhang H (2006) Co-expression of the *Suaeda salsa* SsNHX1 and Arabidopsis AVP1 confer greater salt tolerance to transgenic rice than the single SsNHX1. Mol Breed 17(4):341–353. https://doi.org/10.1007/s11032-006-9005-6